2014 IEEE International Conference on Robotics & Automation (ICRA)
Hong Kong Convention and Exhibition Center
May 31 - June 7, 2014. Hong Kong, China

3D Path Planning of a Laser Manipulation Robotic System for Tooth Preparing

Lei Ma, Dangxiao Wang*, Yuru Zhang, Lei Wang, Peijun Lv, Yuchun Sun

***Abstract*—In this paper, we proposed a 3D path planning method for a miniature robotic system, which can manipulate a beam of ultra-short pulse laser to cut a decayed tooth to formulate an expected 3D shape. Using high resolution STereo Lithography (STL) models of the original decayed tooth and the target preparing shape as the input, our method consists of a fast slicing algorithm and an optimized path generating algorithm, which realized a high efficient layer-by-layer cutting for laser ablation. Theoretical analysis on the geometric distortion and surface roughness was carried out to model the influence of the path planning algorithms on the accuracy of the prepared tooth. Experimental results on a real tooth indicate that the path planning method can maintain the accuracy for the laser ablation process.**

I. INTRODUCTION

Tooth preparing is a fundamental process of the treatment on dental hard tissue disease in dental clinical operations, the objective of which is to remove decayed tissues from a decayed tooth and shape the remaining normal part into an expected shape for further treatment. Fig. 1 shows the process of tooth preparing. In current clinical tooth preparing, there are two typical methods, namely grinding by using turbine-driven drills and ablation by Er:YAG or Er,Cr:YSGG lasers. These two methods not only have poor accuracy but also generate mechanical and thermal stress, thus creating micro cracks of several tens of microns in the enamel [1, 2]. These cracks are starting points for new carious attacks and have to be avoided for long term success of the dental treatment.

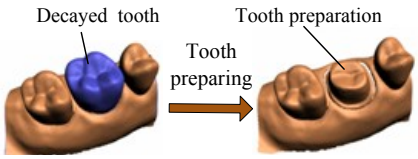

Fig. 1 The process of tooth preparing

In recent years, ultra-short pulse lasers have been introduced into dental surgery, and research results demonstrated that ultra-short pulse laser can be used as a safe and effective tool for clinical tooth preparing [3-8]. In order to overcome the drawbacks of traditional treatment methods, we have developed a miniature robotic system for tooth preparing, which can manipulate a beam of ultra-short pulse laser to shape a target tooth into a tooth preparation [9]. Our long-term goal is to realize automatic tooth preparing in clinical operations using ultra-short laser.

In this paper, we mainly focus on the path planning of the robotic system for the automatic tooth preparing operation. The purpose of the path planning is to generate a 3D path of the laser focus, which can shape a target tooth into an expected 3D tooth preparation. In automatic tooth preparing operation, a layer-by-layer cutting method is proposed to generate a tooth preparation, and a 3D path planning is developed based on this cutting method using STL models of the original decayed tooth and the target preparing shape, which mainly has two processes, slicing and path generating.

Currently, there are some slicing algorithms and path generating algorithms which have been used in rapid prototyping field and laser cutting field. In [10], a fast slicing algorithm was developed based on the grouping matrix and the active triangle table. An algorithm for rapid slicing of ST L model based on sorting by triangle adjacency in layers is proposed, which establishes adjacency relationship between triangle meshes by adopting method of adjacency insertion [11]. P. Wen et al. proposed a fast slicing algorithm based on recursion and searching direct graph with weight [12]. M. Xie et al. developed a path generating algorithm for robot rapid prototype; in this algorithm, double cycling linked lists are used to indicate boundary of a connected region, and then the region will be several monotonous areas to generate optimized path [13]. Q. Zhao et al. provided a tool path generation approach for NC based on an offset method [14].

In automatic tooth preparing operation, the expected accuracy of the tooth preparation is less than 30um, so the resolution of the STL model should be less than 10um, which results in a large number of facets (more than 5×10^5) in the STL Models used for the robotic system. Also, the efficiency of the operation is required to be less than 30min, so effective cutting path is required to enhance the efficiency as well. Meanwhile, the 3D shape of the tooth model is irregular, which generates complex slice contours consisting of multiple unconnected regions.

Lei Ma, Dangxiao Wang, Yuru Zhang and Lei Wang are with the State Key Lab of Virtual Reality Technology and Systems, Beihang University, Beijing, 100191, China.

*corresponding author: hapticwang@buaa.edu.cn

Peijun Lv and Yuchun Sun are with the School and Hospital of Stomatology, Peking University, Beijing, China.

Traditional 3D path planning strategies cannot be directly applied to the automatic tooth preparing process because of the reasons mentioned above. In this paper, we proposed a new 3D path planning strategy which consists of a new slicing algorithm and an optimized path generating algorithm. This strategy can generate an optimized laser cutting path for complex slice contours with fast speed and simple structure. Experimental results of the automatic tooth preparing validate the proposed path planning strategy.

The remainder of the paper is organized as follows. In section II, the miniature robotic system is introduced. In section III, a 3D path planning strategy based on STL model is described, including a last slicing algorithm and an optimized path generating algorithm. In section IV, the accuracy of the path planning is analyzed, and methods are proposed to enhance the accuracy. In section V, automatic tooth preparing experiments are carried out to verify the performance of the proposed path planning strategy. In section VI, conclusion and future work are presented.

II. Laser Manipulation Robotic System

A. Laser manipulation robotic system

As shown in Fig.2, the laser manipulation robotic system includes the following components: a miniature robotic end-effector, a tooth fixture, a laser generator, a laser transmission arm, a laser scanner and a computer console. The miniature robotics end-effector will be installed on the transmission arm, and then connected and fixed on the tooth fixture, thus maintaining no relative motion between the end-effector and the target tooth during tooth preparing.

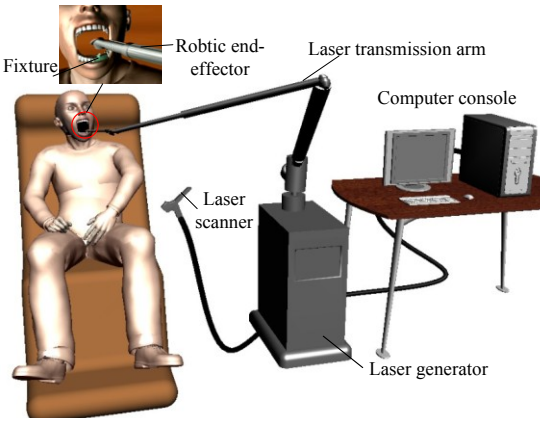

Fig. 2 Conceptual illustration of the automatic tooth preparing system

In the beginning of the automatic tooth preparing operation, the 3D cutting path of the laser focus is first generated in the host computer based on the STL files of the target tooth and the tooth preparation, which is the key process of the automatic tooth preparing system. Then the tooth fixture and the miniature robotic end-effector are inserted into a patient's oral cavity. Finally, the laser focus will be controlled by the robotic end-effector to track the cutting path, and shape the target tooth into the tooth preparation.

B. The miniature robotic end-effector

The function of the miniature robotic end-effector is to control the movement of the laser focus in three-dimensional space, and the robotic end-effector mainly has three components: an optical system, a mechanical system and a control system.

As shown in fig.3, the optical system consists of a vibrating mirror X, a vibrating mirror Y, a protruding optical lens, and a reflecting mirror. When a parallel laser beam is emitted from a laser generator, and transferred to the scanning system through the transmission arm, the vibrating mirrors X, Y will change the beam's direction in sequence and then sends it into the protruding optical lens. Passed through the lens, the beam becomes a focal laser, and then the focused laser reflected by a static mirror will exactly strike on the surface of a tooth by selecting an appropriate distance between the tooth and the lens. [9].

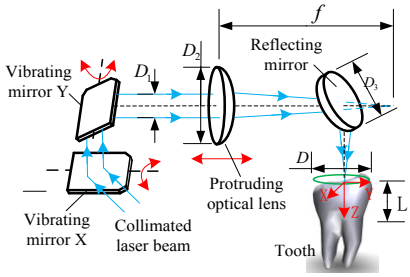

Fig. 3 Optical components and transmission path of the laser beam

There are three moving optical components in the mechanical system of the robotic end-effector, including two vibrating mirrors and a protruding optical lens. As shown in Fig.4, these three parts are driven by motors directly: the two vibrating mirrors are driven by pendular motors, and the protruding optical lens is driven by a linear motor. According to the layer-by-layer cutting method, the movement of the vibrating mirrors and the movement of the protruding optical lens are independent. Therefore, the vibrating mirrors and the protruding optical lens are controlled independently in order to simplify the control system of the end-effector.

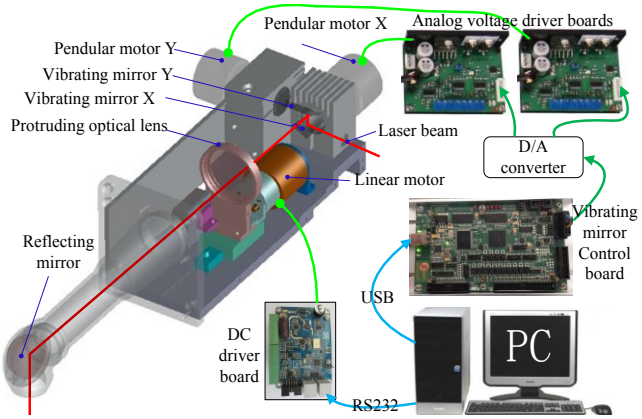

Fig.4 Mechanical system and control system of the robotic end-effector

C. STL models for path planning

In order to achieve a high accuracy tooth preparation, the redundant tooth tissue of the target tooth needs to be removed accurately. Therefore, a high resolution geometric model of the removal tooth tissue is needed to create laser cutting path. As shown in Fig.5, the geometric model of the removal tooth tissue is obtained by subtracting the model of the tooth preparation with the model of the target tooth. The geometric model of the target tooth is achieved using a laser scanner and stored as STL files, and the geometric model of the tooth preparation is designed using Mimics (Materialise Mimics 10.0, STL Module) based on the model of the target tooth, also stored as STL files. STL is a file format which describes the surface geometry of a three dimensional object using triangular facets.

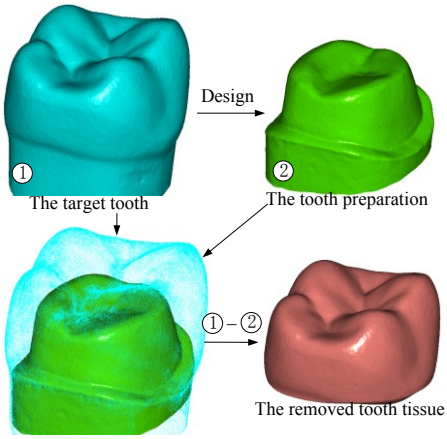

Fig.5 Obtaining the geometric model of the removed tooth tissue

D. Safety issues

The safety is an important part of the proposed robotic system, since the system is used to remove tooth tissue in oral cavity which has kinds of soft tissue. In this medical system, there are two precautions taken to ensure the safety during the tooth preparing process. One is using the tooth fixture, which is fastened to target tooth as shown in Fig.6, to fix the robotic end-effector, so that the position between tooth and end-effector can be kept unchanged, which can protect adjacent teeth and soft tissue of the oral cavity. Another precaution is using a CCD camera to monitor the tooth preparing process, and based on the video the camera provides doctors can stop the process when an emergency happens

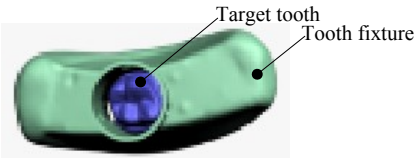

Fig. 6 No relative motion between the tooth fixture and the target tooth

III. Path Planning Algorithm

In order to meet the requirements of the automatic tooth preparing operation, a 3D path planning strategy is proposed based on the layer-by-layer cutting method. The strategy consists of a fast slicing algorithm and an optimized path generating process, and the STL model used for the strategy is a high resolution model of the removal tooth tissue.

A. Fast slicing algorithm

The purpose of the slicing process is to transform a complex three-dimensional topography of the STL model into simple two-dimensional slice contours. And the path generating process is based on these slice contours. In previous slicing algorithms, a directed closed slice contour was generated [10,11], so it was needed to construct the topology relationship of the facets in STL model or sort the intersection points, thus limiting the efficiency of these slicing algorithms. In this paper, we propose a fast slicing algorithm, which can generate an undirected closed slice contour, simplifying the slicing process and improving the slicing speed.

In the first step, all the triangle facets in the STL model are divided into groups, and the grouping method is as following. For each triangle facet, calculation is made to figure out the slice planes that the facet intersects with based on the coordinate value of the first slice plane and the spacing of the adjacent slice planes. In the proposed slicing algorithm, the spacing between two adjacent slice planes, i.e. the slice thickness, is equal. Then, these triangle facets which intersect with the same slice plane are divided into one group. Based on the proposed grouping method, the grouping can be completed by traversing all the facets only once. In each group, the facets are continuous because the STL model of the removed tooth tissue is closed.

The next step is to generate an undirected closed slice contour. As shown in Fig.7, a slice plane intersects with 6 facets, and every facet will produce an intersection segment. We can find that six intersection segments form an undirected contour line. Therefore, an undirected closed slice contour will be generated due to the continuity of the triangle facets in each facets group created in the first step.

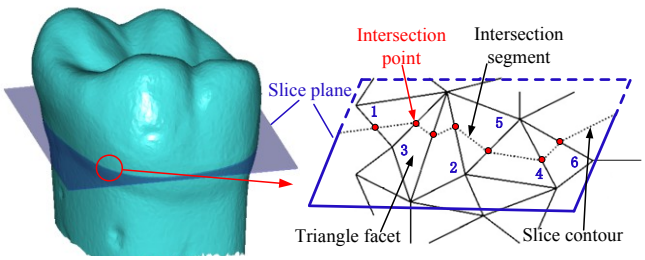

Fig.7 The diagram of generating slice contour

B. Optimized path generating algorithm

The optimized path generating process is carried out based on these slice contours created in the slicing process. Filling lines are first used to calculate laser cutting points. In this paper, we assume that the filling lines are parallel to the Y axis. As the slice contour consists of a large number of unordered segments, the calculation method is proposed as follow. For each segment, the first step is to figure out the filling line that the segment intersects with based on the

coordinate value of the first filling line and the spacing of the adjacent filling lines. Then the intersection point will be calculated, and all the intersect points will be stored in a points list at last.

The second step is to sort the intersection points to generate laser cutting lines. As shown in Fig.8, there are three regions in a slice contour: region 1 is a cutting region which will be filled with laser cutting path, while region 2 and region 3 are not cutting regions. It is clear that the number of the intersection points on a single filling line is an even number, and lines from the odd point to the even point is the laser cutting path. According to the analysis above, the sorting method is illustrated as follow: all the intersection points are sorted based on the X value of the points in the ascending order. Then, for these intersection points whose corresponding filling line is the same one, they are sorted again based on the Y value of the points in the ascending order. After the sorting process, a new points list is created, the line segments between the 2m-1(m is an integer and larger than zero) point and the 2m point are the laser cutting lines, and all the laser cutting lines are continuous.

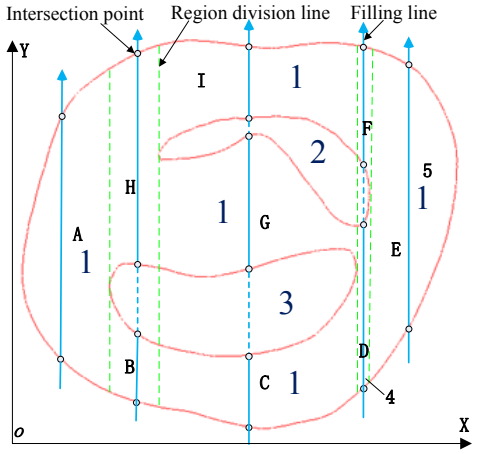

Fig.8 The diagram of the filling lines intersecting with slice contour

The third step is to generate optimized laser cutting path. As shown in Fig.8, the cutting region 1 is divided into several small cutting areas (A~ I) depending on the different number of intersection points of a single filling line. Area A, B, C, D and E consist of the laser cutting lines which are formed by the first intersection point and the second point on the same filling line, so these five areas are continuous. Area F, G and H are formed by the third intersection point and the fourth point, and I area is formed by the fifth point and the sixth point. So an optimized laser cutting path is generated from area A to area I in alphabetical order as shown in Fig.9 based on the following principle: The laser path lines formed by the first intersection point and the second point on the same filling line are cut firstly, then the laser path lines formed by the third intersection point and the fourth point. And continue this process until all the laser cutting lines are traversed. And lines between two areas are jumping lines.

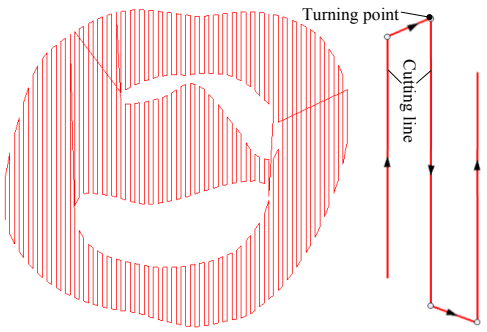

Fig.9 The optimized laser cutting path of a slice contour

As shown in Fig.9, there are lots of turning points in the path, and the motors that drive the reflecting mirrors must slow down and change rotational direction at the turning point so that the laser beam can reach the turning point exactly. Meanwhile, the mirrors have inertia, which mean that the mirrors should need a delay in order to move accurately. Therefore, the mirrors need a delay called inflexion delay to change rotational direction and reach the turning points accurately in general application, which results in increasing the total time of tooth preparing process. In future work, this issue will be discussed.

ACCURACY AND ROUGHNESS OF THE PATH PLANNING

In clinical tooth preparing operation, the shape accuracy of the final prepared tooth includes two requirements: the linear error is required to be less than 0.1mm, and the error of the convergence angle [15] is required to be less than 2~5°[16]. These two parameters are main evaluation indicators to judge the quality of the tooth preparation. Meanwhile, the surface of the tooth preparation is required to be smooth. In the automatic tooth preparing automatic operation, path planning directly determines the accuracy of the tooth preparation, so the accuracy of the path planning is analyzed in this section.

The layer-by-layer cutting method is employed in the automatic tooth preparing operation, so multistep-like behavior will be generated inevitably as shown in Fig.10. The multistep-like behavior will cause the geometric distortion of a tooth preparation and influence the surface roughness.

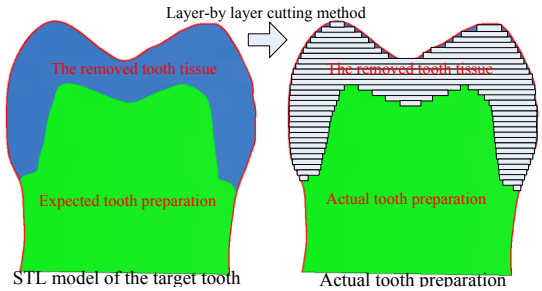

Fig.10 Multistep-like behavior created by the layer-by-layer cutting method

C. *Geometric distortion*

Geometric distortion generated by multistep-like behavior, mainly influencing the linear error, has relationship with the slicing thickness, the slicing direction and the normal vector of the model surface. Smaller slice thickness and smaller

acute angle between the slicing direction and the normal vector of the model surface can reduce the geometric distortion. Meanwhile, as shown in Fig.11, the actual tooth preparation will be inscribed in the expected tooth preparation if the angle between the slicing direction and the normal vector of the model surface is obtuse, and the actual tooth preparation will be larger than the expected tooth preparation if the angle between the slicing direction and the normal vector of the model surface is acute as well.

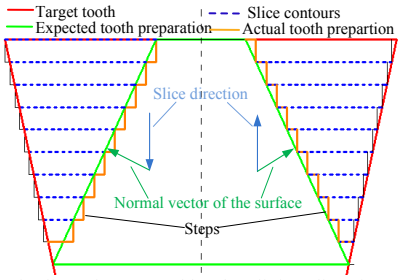

Fig.11 Geometric distortion caused by the slicing direction and the normal vector of the model surface

In order to evaluate the geometric distortion, the volume distortion degree is used as a key indicator. The equation of the volume distortion degree can be derived as

$$k_v = V_r / V_{stl} \tag{1}$$

where V_{stl} is the volume of the expected tooth preparation, and V_r is the volume of the actual tooth preparation. The volume of the actual preparation is calculated based on the equation

$$V_r = \sum_{i=1}^{n} S_i \Delta h \tag{2}$$

where S_i is the area of the cutting region in a slice contour and can be obtained on the basis of the path generating process, and Δh is the selected slice thickness in the slicing process.

D. Surface roughness

Multistep-like behavior can create steps on the surface of the actual tooth preparation, and these steps have a bad effect on the surface roughness of the actual tooth preparation. In automatic tooth preparing operation, the surface roughness mainly depends on the height of the steps. The higher the steps are, the larger the surface roughness will be. Fig.12 shows the diagram of the surface of the actual tooth preparation. A step AB generates a surface peak at A point and a surface valley B point by the surface middle line, and the distance between A point and the surface middle line will be the height of the surface peak. Therefore, Z_p, the height of the surface peak at A point, can be calculated using the equation:

$$Z_p = \frac{\Delta h}{2} \times \cos\beta \tag{3}$$

where Δh is the height of the step, and β is the angle between the normal vector of the surface at A point and Z axis.

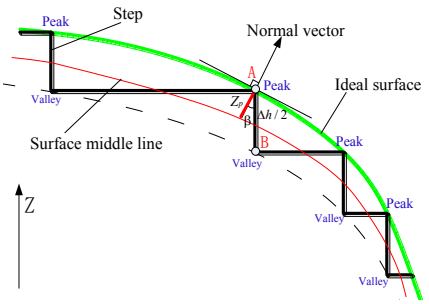

Fig.12 The surface of the actual tooth preparation

From the equation (3), we can conclude that the surface roughness of the actual tooth preparation depends on the height of the steps Δh and the angle β. For the surface of the tooth, the range of the angle β is from $0°$ to $90°$. Therefore, the maximum step height of the surface peak on the surface of the tooth preparation is $\Delta h / 2$, so the surface roughness of the tooth preparation is not more than $\Delta h / 2$.

E. Methods to the improve the accuracy and roughness

Based on the analysis above, the height of the steps, the slicing direction and the normal vector of the tooth surface are the key factors which influence the geometric distortion and the surface roughness. For a particular tooth, the normal vector of its surface is a fixed value. Therefore, the other factors are studied to improve the accuracy of the tooth preparation.

Since the height of the steps not only influences the geometric distortion but also determines the surface roughness, the accuracy will be improved if the height of the steps can be reduced. In the laser tooth preparation system, the height of the steps is equal to the selected slice thickness, so smaller slice thickness can be set to reduce the step height theoretically. However, smaller slice thickness will cause the protruding optical lens to move frequently, and the cumulative error of the motion control will also increase, thus reducing the efficiency and accuracy of the tooth preparing process. In the robotic end-effector, the focal distance of the lens that used in the device is 157mm, which results in the focal length to be 1mm, and we found that the removal thickness of monolayer remains almost the same around 100um of the focal plane. According to experimental data, the removal thickness of monolayer is about 10um (laser power is 3w, cutting speed is 169mm/s, repetition frequency is 10 KHz). Based on these features, a method is first proposed to reduce the height of the steps, despite the influence and the efficiency requirements: the slice thickness is set to the monolayer cutting depth, and the protruding optical lens moves once after a certain number of the slice contours are cut. The moving length of the optical lens at every time should be less than 100um, so the certain number can be calculated.

While the slice direction has a bad effect on the geometric distortion no matter what the slice direction is, a compensation method is proposed in order to reduce the

effect of the slice direction on geometric distortion as shown in Fig.13. In this method, the coordinate value of the first slice plane will add or subtract a compensation amount based on the selected slice direction, and the compensation amount is half of the slice thickness. Obviously, this method can reduce the geometric distortion.

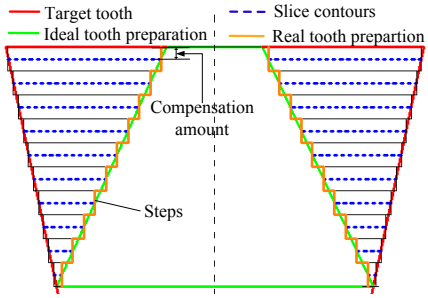

Fig.13 A compensation method for the slice direction

IV. EXPERIMENTS

In this section, experiments were carried out to verify the performance of the proposed 3D path planning strategy. As shown in Fig.14, an experiment platform was established: a laser beam was emitted from the laser generator, and then the laser beam stroked the vibrating mirror X horizontally, and finally the laser bean would be a focal laser on the surface of an experimental material which was fixed on a three-dimensional translation stage. The laser generator is a picosecond laser (Maximum output power 10w, maximum repetition frequency 10 kHz, pulse width 15ps, wavelength 1064ns).

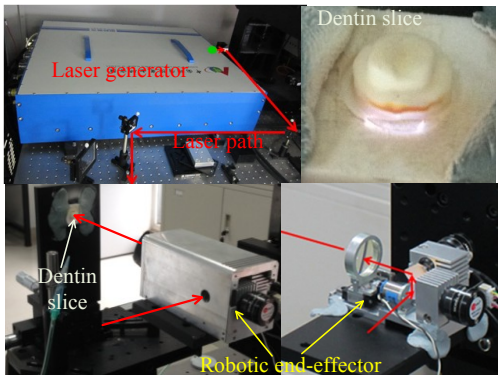

Fig.14 Experiment platform

Generally, it is hard to find the exact location of the focus because the focal length is too long. In the experiments, we moved the translation stage manually at low power. And then we measured the diameter of the laser focus to be 33.8um.

A. Cutting Experiment of 2D slice contours

At first, a cutting experiment of 2D slice contour was carried out to verify the optimized path generating algorithm. The experiment was designed to cut two complex two-dimensional slice graphics on a colored hard paper. The distance between two adjacent filling lines was set to 33.8um in order to ensure the zero overlapping ratio of the cutting lines, and the scanning speed is also set to 338mm/s. Experimental results are shown in Fig.15, we can find that the whole cutting areas are scanned entirely without missing lines, so we can conclude that the optimized path generating algorithm is correct.

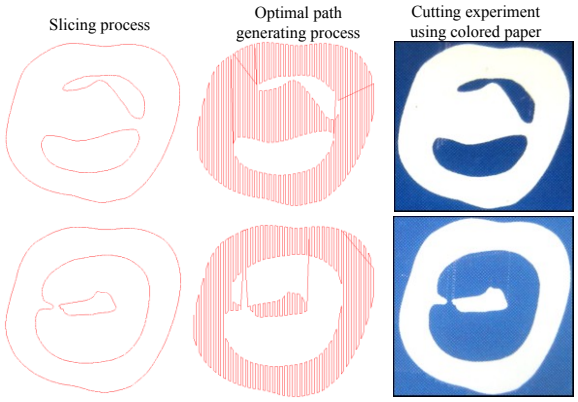

Fig.15 Results of cutting experiment of 2D slice contours

B. Automatic tooth preparing experiment

The tooth tissue is not homogeneous with multiple components like enamel and dentin, and this unevenness may affect the verification. In order to reduce the tooth's non-homogeneity effect, the tooth used in this experiment was preprocessed to remove the enamel and retain the dentin as the experiment material.

In this experiment, the first step was to achieve the monolayer cutting depth of the dentin under the specific laser parameter. As shown in Fig.16, we designed a cutting method: there were five slice contours which were rings with different diameters, and each slice contour was cut five times from the largest one to the smallest one, and finally a circular cone with steps was generated. The optical lens remained still in the whole process. After ablation, we measured the height of every step, and then got the average height of the five steps, which was five times of the monolayer cutting depth. In this experiment, the laser parameters (output power 3.0w, repetition frequency 10 kHz) were selected for this experiment, and the cutting speed were 169mm/s. The average height of the five steps achieved in the experiments is 46um, which means the monolayer cutting depth of the dentin is 9.2um.

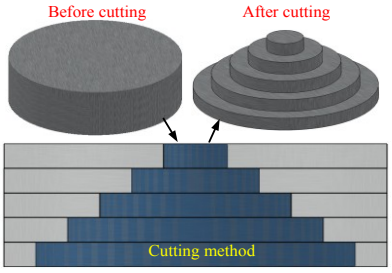

Fig.16 A cutting method is proposed to achieve the monolayer cutting depth

Based on the monolayer cutting depth, a tooth preparing experiment based on dentin was carried out. The slicing thickness was set to 9.2um, and the number of slicing plane was set to 500, so the target depth should be 4600um. The

target convergence angle of the expected tooth preparation was 16.38° . A single feed amount of the optical lens was set to 46um according to the five times of the monolayer cutting depth, i.e., the lens would move once after the laser cut five slice contours.

As shown in Fig.17, a tooth preparation was generated in the experiment. The time of the experiment is 3.5 hours. The actual convergence angle is 15.86°, so the angular error is 0.5°. As shown in Fig.18, model matching was carried out to measure the three-dimensional shape error using the STL models of the actual tooth preparation and the expected tooth preparation. According to the measurement, the maximum error is 0.145mm, and the average error is 0.05mm.

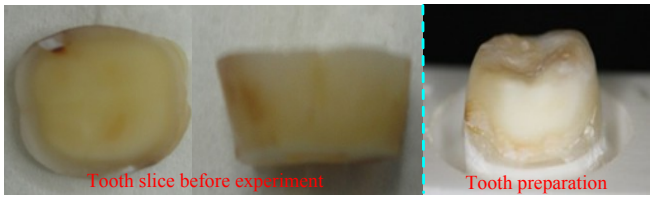

Fig.17 A tooth preparation generated in the experiment

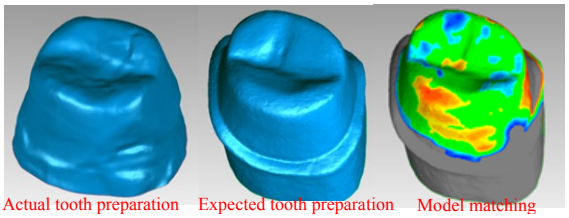

Fig.18 Model matching to measure the accuracy of the tooth preparation

From the result of the laser tooth experiment, we can conclude that the proposed 3D path planning method can generate a target tooth preparation. Meanwhile, some problems need to be solved in the future work. Firstly, the maximum three-dimensional shape error of the actual tooth preparation is 0.145mm and larger than 0.1mm, which does not perfectly meet the tooth preparing requirement. Besides, the current ablation efficiency is too low, relative to the expected time half an hour, so more powerful laser generator and more efficient ablation method are required in future to improve the efficiency issue.

V. Conclusion and Future Work

Based on high resolution STL models of the original decayed tooth and the target preparing shape, a 3D path planning strategy was proposed for automatic tooth preparing operation in this paper, including a fast slicing algorithm and an optimized path generating algorithm. In the fast slicing algorithm, an undirected closed slice contour was generated to substitute a directed closed slice contour which generated by traditional slicing algorithm, and thus to improve the efficiency of the slicing process. In the proposed optimized path generating algorithm, lines filling method is used to achieve the laser cutting lines, and an optimized path is generated by dividing a complex slice contour into small independent areas. Finally, experiments were designed to evaluate the performance of the 3D path planning strategy, and results indicated that the strategy is correct and feasible to generate a tooth preparation on a target tooth. Limitations and future work are also put forward according to the automatic tooth preparing experiment results.

Acknowledgment

This work is supported by the National Key Technology R&D Program of China under the grant No. 2012BAI07B04, and by the National Natural Science Foundation of China under the grant No. 61170187.

References

[1] H. Wigdor, J. T. Walsh, and S. R. Visuri. “Dental material ablation with the Er: YAG laser,” Lasers and Electro-Optics Society Annual Meeting, 1994, LEOS'94 Conference Proceedings. IEEE. Vol. 2: 73-74.

[2] A. Aoki, I. Ishikawa, T. Yamada, M. Otsuki, H. Watanabe, et al., “Comparison between Er: YAG laser and conventional technique for root caries treatment in vitro,” Journal of dental research 77.6 (1998): 1404-1414.

[3] B. Schwab, D. Hagner, W. Müller, H. Lubatschowski, T. Lenarz, and R. Heermann, “Bone ablation using ultra-short laser pulses. A new technique for middle ear surgery,” Laryngo-rhino-otologie, 83.4 (2004): 219-225.

[4] J. Krüger, W. Kautek, H. Newesely, “Femtosecond-pulse laser ablation of dental hydroxyapatite and single-crystalline fluoroapatite,” Applied Physics A, 1999, 69(1): S403-S407.

[5] J. Serbin, T. Bauer, *C.* Fallnich, “Femtosecond lasers as novel tool in dental surgery”, applied surface science, 2002, 197: 737-740.

[6] R. F. Z. Lizarelli, M. M. Costa, E. Carvalho-Filho, “Selective ablation of dental enamel and dentin using femtosecond laser pulses,” Laser Physics Letters, 2008, 5(1): 63-69.

[7] A. Daskalova, S. Bashir, W. Husinsky, “Morphology of ablation craters generated by ultra-short laser pulses in dentin surfaces: AFM and ESEM evaluation,” Applied Surface Science, 2010, 257(3): 1119-1124.

[8] J.F. Kraft, K. Vestentoft, B.H. Christensen, et al, “Calculus removal on a root cement surface by ultra-short laser pulses”, Applied Surface Science, 2008, 254(7): 1895-1899.

[9] L. Wang, D.X. Wang, L.Ma, Y.R. Zhang, F.S. Yuan, et al., “Preliminary experiments of a miniature robotic system for tooth ablation using ultra-short pulsed lasers,” Intelligent Robots and Systems (IROS), 2013 IEEE/RSJ International Conference on. IEEE, 2013: 2566-2571.

[10] Y. Wu, B. Zhao, and S. Wang, “Algorithm for rapid slicing STL model,” Journal of Beijing University of Aeronautics and Astronautics 4 (2004): 329-333.

[11] S. Wang, H. Liu, and X. Zhu, “An Algorithm for Rapid Slicing of STL Model Based on Sorting by Triangle,” Jour n al of Computer Aided Design & Computer Graphics 21.4 (2001): 600-606

[12] P.Z. Wen, W.M. Huang, and C.K. Wu, “Modified fast algorithm for STL file slicing,” Journal of Computer Applications 28 (2008): 1766-1768.

[13] M. Xie, C. Li, Z. Shao, “The Section-filling and Path Plan on the Robot Rapid Prototype (RRP),” Machine Design and Research 3 (2000): 007.

[14] Q.S. Zhao, X.H. Huang, Chao Wang, et al, “NC tool path generation approach based on STL,” IT in Medicine and Education (ITME), 2011 International Symposium on. IEEE, 2011, 2: 228-231.

[15] S. Mou, T. Chai, J. Wang, and Y. Shiau, “Influence of different convergence angles and tooth preparation heights on the internal adaptation of Cerec crowns," The Journal of prosthetic dentistry 87.3 (2002): 248-255.

[16] J. Xu, J. Yuan, Z. Wang, “Prosthetic dentistry,” Beijing, People's Military Surgeon Press, 2001.4 (In Chinese).